Hindawi
Journal of Nanomaterials
Volume 2018, Article ID 6482186, 8 pages
https://doi.org/10.1155/2018/6482186

Research Article

Synthesis, Characterization, and Catalytic Activity of Platinum Nanoparticles on Bovine-Bone Powder: A Novel Support

S. A. Gama-Lara,[1] Raúl. A. Morales-Luckie,[1] L. Argueta-Figueroa,[1] Juan P. Hinestroza,[2] I. García-Orozco,[1] and R. Natividad[1]

[1]*Centro Conjunto de Investigación en Química Sustentable UAEM-UNAM, Carretera Toluca-Atlacomulco Km 14.5, San Cayetano, 50200 Toluca, MEX, Mexico*
[2]*Department of Fiber Science and Apparel Design, Cornell University, 242 Van Rensselaer Hall, Ithaca, NY 14853-4203, USA*

Correspondence should be addressed to Raúl. A. Morales-Luckie; ramluckie@gmail.com and R. Natividad; reynanr@gmail.com

Received 23 June 2017; Revised 4 January 2018; Accepted 21 January 2018; Published 13 March 2018

Academic Editor: Jorge Pérez-Juste

Pt nanoparticles supported on bovine-bone powder were obtained by a rather simple method consisting of immersing powder of bovine bone into a Pt^{+4} metal ion solution at room temperature and subsequent reduction by sodium borohydride. This method eliminates the calcination step of the usual catalyst preparation methods. The nanocomposite was characterized by transmission electron microscopy (TEM), which revealed uniformly dispersed platinum nanoparticles with average particle size of 2.2 nm ± 0.6 nm. The XPS studies exhibited the presence of 63% Pt° and 37% PtO. The catalytic activity was tested in the hydrogenation of 2-butyne-1,4-diol. The nanocomposite shows good catalytic performance with nearly 100% conversion and 83% selectivity towards 2-butene-1,4-diol.

1. Introduction

Science and technology of nanomaterials have rapidly grown in recent years and, as a consequence, great progress in the synthesis and characterization of materials in the nanometer regime has been achieved. The applications of these nanomaterials are diverse in the chemical industry, in electronics, and even in medicine [1, 2]. One of the main applications of nanomaterials, however, is in catalysis. This is due to the positive impact that high superficial area of nanoparticles exerts on reaction time, costs, and process efficiency [1, 3–7]. However, in order to prevent sintering and have an easy recovery of the catalyst from the reaction medium, supports are employed. Carbon, titania, metal-organic frameworks, graphene, mesoporous silica, or various polymers have been successfully applied as supports by several research groups [8–18].

The conventional nanoparticle synthesis is complex and relatively expensive and is conducted at high temperatures. These undesirable features have motivated the search of a greener synthesis. To achieve so, the general approach that can be found in the literature is by modifying the reaction medium to produce the nanoparticles, mainly in the liquid phase [19–23]. Little has been said though about the role of the biosupports in controlling the shape and size of synthesized nanoparticles. In this context, the use of natural, renewable, abundant, and low-cost material supports is desirable for metal nanoparticles controlled synthesis. The use of biosupports allows a room temperature synthesis and the use of aqueous medium. This opens a rather interesting area for synthesis from a green and sustainable technology point of view. In this sense, living organisms show an amazing hierarchical arrangement of their organic and inorganic components, from the nanoscale to the macroscopic scale. Many of them are porous materials (including wood, cork, bone, ivory, and shells) with high prospective to be employed as nanoreactors and/or templates to attach metallic structures with nanometric dimensions [24, 25]. In this context, Lin et al. have reported the one-step synthesis of platinum nanoparticles supported on wood, using hydroxyl groups (OH^-) as reducing agent, to obtain a nanomaterial with high and relatively stable activities in the catalytic reduction of *p*-nitrophenol [26].

Devia and Mandal reported the self-assembly of Ag nanoparticles using hydroxypropyl cyclodextrin for the catalytic reduction of p-nitrophenol [27]. Actually, cellulose has been studied as template since it is a natural carbohydrate rich in oxygen containing anhydroglucose units, linked by hydrogen bonds to form nonlinear molecular chain [28]. Bones, nonetheless, are constituted mainly by hydroxyapatite, which exhibits donor OH^- and $PO_4{}^{-3}$ groups to anchor metallic ions.

Therefore, the purpose of this study was to synthesize at relatively low cost monodispersed Pt nanoparticles (NPs) onto a bovine bone, which is a renewable and novel biosupport. In addition, the catalytic activity of the as-prepared material was assessed in the hydrogenation catalytic conversion of 2-butyne-1,4-diol to 2-butene-1,4-diol.

2. Experimental Methods

2.1. Pt/Bovine-Bone Synthesis. In order to synthesize the Pt NPs, $PtCl_4$ was used as precursor salt. For this purpose, 16.75 mg of $PtCl_4$ was dissolved in 50 mL of deionized water, thus obtaining a final concentration of 0.001 M (solution 1). Then 7.5 mg of $NaBH_4$ was dissolved in 50 mL of water thus obtaining a 0.01 M concentration (solution 2); pH was not adjusted. For the support bovine femur was used. This bone was washed, cleaned, and immersed in a 0.01 M HCl solution. After immersion, the bone was cut into small pieces and then powdered by a tungsten rotating piece connected to a mototool. The powder was then sieved with 150 mesh. An amount of 975 mg of bovine-bone powder was immersed in 50 mL of solution 1 for 30 seconds and then filtered. The reduction of Pt(IV) ions was carried out with solution 2 for 30 minutes and filtered. The resulting powder was dried overnight at room temperature. It is worth noticing that a calcination step is not necessary since Pt NPs were obtained by $NaBH_4$ as reduction agent. It is also worth pointing out that, because of the amount of treated powder (approximately 1 g), a micellar activity might also be expected since the micelle formation of sepia cartilage collagen solutions has been previously reported [30].

2.2. Characterization. Scanning electron microscopy (SEM) observations were carried out by JEOL JSM-6510LV equipment. The nanocomposite was attached to the sample aluminum-stub using a carbon conductive double-stick tape without coating. Elemental analysis characterization was performed using an energy-dispersive X-ray spectroscope INCA X-Sight Oxford attached to the SEM.

Transmission electronic microscopy (TEM) studies and SAED (selected area electron diffraction) technique were carried out using a JEOL JEM-2100 microscope operating at 200 kV accelerating voltage. The platinum-impregnated bovine-bone powders were suspended in 2-propanol and then ultrasonically dispersed for 5 hours at room temperature. A drop of this suspension was then placed on a Cu-grid coated with a holey carbon film. Also, the supported Pt° nanoparticles were analyzed by STEM technique.

The X-Ray Photoelectronic Spectroscopy (XPS) analysis was carried out in a JEOL JPS-9200 equipped with a Mg source (1253.5 eV), operating at 200 W and vacuum of 1×10^{-8} Torr; for all samples, the analysis area was 1 mm^2. The SpecSurf™ software was used to analyze the experimental results. Charge correction was done based on the adventitious carbon signal (C1s) at 285.5 eV. Shirley method was used for background adjustment, whereas Gauss-Lorentz method was used for curve fitting.

2.3. Hydrogenation of 2-Butyne-1,4-diol. The hydrogenation of 2-butyne-1,4-diol was carried out in a 300 mL stainless-steel Parr reactor equipped with a temperature control system, a mechanical stirrer, a pressure meter, an inner heating/cooling coil system, and sampling valve. A reservoir for H_2 gas was used along with a constant pressure regulator to supply hydrogen at a constant pressure to the reactor.

In a typical hydrogenation experiment, 150 mL of 20% w/w aqueous 2-butyne-1,4-diol solution and 0.215 g of Pt-supported catalyst were loaded into the reactor. The initial concentration of the alkyne was 0.1 mol/L. The reactor was first flushed with nitrogen and then with hydrogen. After the desired temperature (328 K) was reached, the system was pressurized with hydrogen at the required pressure (6 bar) and an agitation speed of 550 rpm. Samples were obtained every 30 minutes. After the reaction was over as indicated by a constant hydrogen pressure in the reservoir, the reactor was cooled down to room temperature, the excess of hydrogen was vented out safely, and the reactor contents were removed for subsequent analysis.

The withdrawn liquid samples were analyzed by gas chromatography with a flame ionization detector using a VARIAN CP3800 GC (DB-WAX 52 column, length 32 m, inner diameter = 0.3 mm) and helium (30 ml/min) as carrier gas, according to previous reported analysis methods [29, 31, 32]. Reaction samples were injected into the GC and analyzed under the following conditions: temperature detector was set at 518 K, injector temperature was set at 513 K, initial oven temperature was 353 K, and this was raised up to 493 K at a rate 10 (K/min). This final oven temperature was kept constant for 3 minutes.

3. Results and Discussion

3.1. Characterization. In this work, in order to prevent sintering and to control nanoparticles size and morphology, the use of a bovine bone was assessed as novel support for Pt nanoparticles (NPs) synthesis. The formation of the metallic platinum phase in solution in the investigated system is the direct result of the transfer of electrons from the reducing agent, $NaBH_4$, to Pt(IV) ions according to reaction [33]:

$$2Pt^{4+} + BH_4{}^- + 4H_2O \longrightarrow 2Pt + B(OH)_4{}^- + 8H^+ \quad (1)$$

Sodium borohydride is a powerful reducing agent, having the ability to completely convert Pt ions into metallic Pt. The size of Pt NPs is controllable by varying the time of immersion of bovine bone into the Pt (IV) solution. The immersion time was a variable of study, and 30 seconds of immersion time was found to be the optimal for the NPs synthesis. It was observed that the size of Pt NPs was smaller at shorter times. Besides, a significant improvement on particle size was observed by increasing the support area (achieved by powdering the bovine bone).

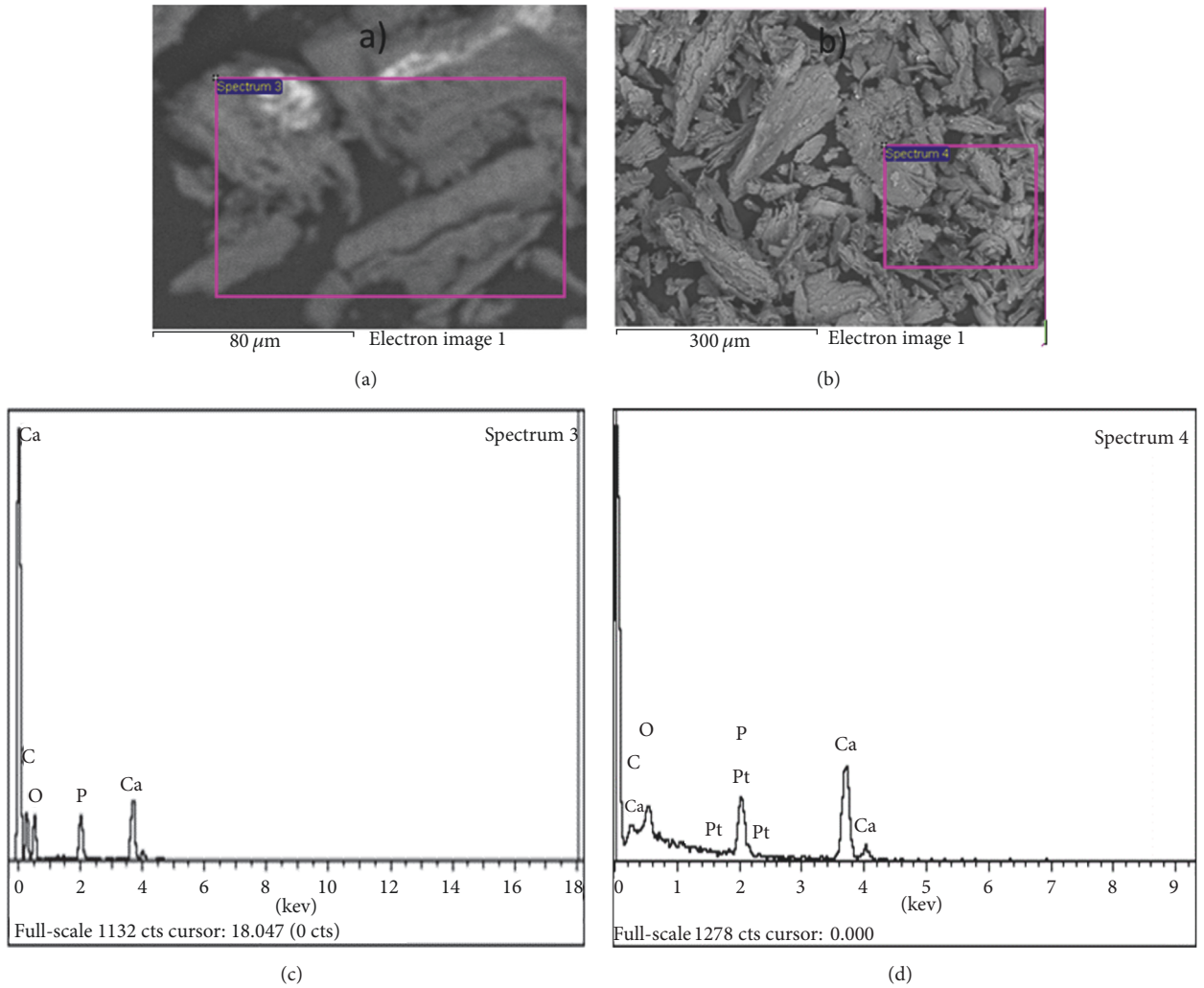

Figure 1: (a) SEM image of bovine-bone powder, 20 kV. (b) SEM image of bovine-bone powder after the synthesis of nanoparticles of platinum, 20 kV. (c) EDS spectrum: the analyzed area is indicated by the pink square. ((a) and (d)) EDS spectrum: the analyzed area is indicated by the pink square in (b).

When bone in bulk was used, micrometric rather than nanometric size Pt particles were obtained. This fact could be explained by the ability of bone powder to avoid the platinum ions agglomeration, since there is a large distance between metal ions. Bovine-bone powder is an ideal substrate for the formation of nanoparticles due to its high porosity (200–900 μm) and high superficial area. In addition, the chemical structure of bone tissue has a high electronic density provided by OH^- and PO_4^{-3} groups.

In Table 1, the presence of the main elements that constitute the hydroxyapatite in bovine bone can be observed. Figures 1(a) and 1(c) show the SEM micrograph and EDS spectrum of bovine powder without treatment, respectively. Figure 1(b) shows a SEM image of bovine-bone powder after the impregnation with the Pt NPs. In addition, the EDS spectrum in Figure 1(d) shows the presence of hydroxyapatite elements and Pt.

The supported Pt NPs were further identified by STEM. Figure 2 shows the presence of the Pt NPs all over the surface of the bovine-bone powder, which could be linked by electrostatic forces between Pt (+) and the support (hydroxyapatite OH^-). Figures 2(a), 2(b), 2(c), and 2(g) reveal that quasi-spherical Pt NPs with low size polydispersity are obtained into the bovine-bone surface. These images correspond to a randomly chosen part of the substrate and can be considered as representative of the overall size and shapes of the particles.

Table 1: Elemental weight% for EDS elemental analysis of Figures 1(a) and 1(b).

Element	Elemental weight% of bone	Elemental weight% of bone/Pt NPs
C K	15.78	15.18
O K	42.98	41.15
P K	13.08	12.41
Ca K	28.16	27.56
Pt M	---	3.71

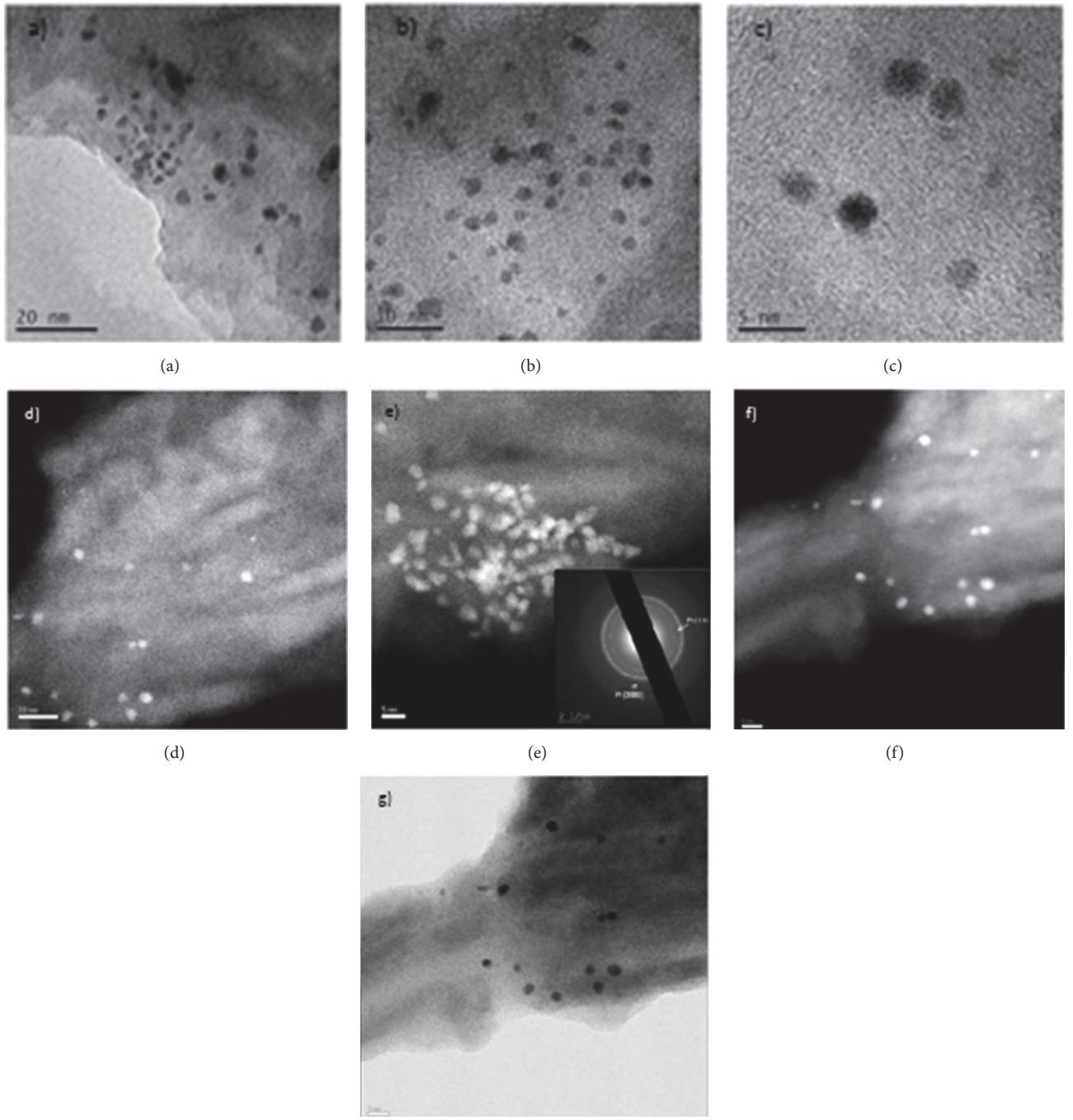

(a) (b) (c)

(d) (e) (f)

(g)

Figure 2: ((a), (b), (c), and (g)) BF-STEM images of Pt nanoparticles in bovine-bone powder, in different magnifications 200 kV. ((d), (e), and (f)) HAADF-STEM images of supported Pt nanoparticles on bovine-bone powder.

Images depicted in Figures 2(d) and 2(e) were generated by high angle annular dark-field scanning transmission electron microscopy (HAADF-STEM). These images correspond to Pt nanoparticles on the bovine-bone powder after 5 hours of ultrasonication. Figures 2(f) and 2(g) illustrate the difference between the HRTEM and the HAADF and show the difference of electronic density between the Pt NPs and the bone powder support. Selected area electron diffraction (SAED) image shows spots corresponding to (111) and (200) reflections of Pt NPs lattice planes, which confirms the FCC symmetry (Figure 2(e)). This indicates polycrystalline Pt NPs.

Mei et al. [34] prepared platinum nanoparticles in Spherical Polyelectrolyte Brushes by $NaBH_4$ chemical reduction, where the surface anions of the support act as an anchor for the Pt (IV) ions and thiols were used to avoid aggregation

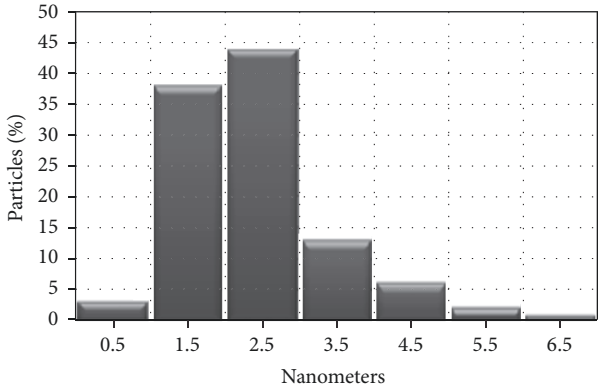

Figure 3: Size distribution of platinum nanoparticles.

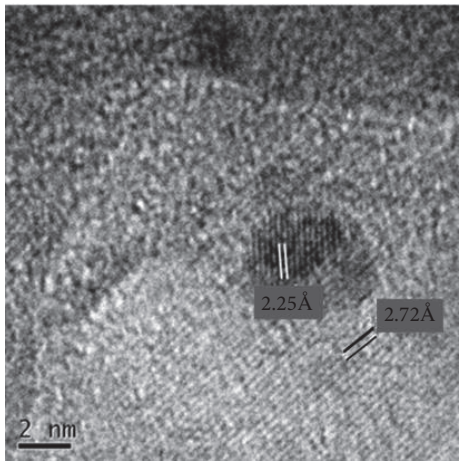

Figure 4: HRTEM micrograph Pt-nanobiocomposite.

of Pt particles. However, in this work, it is proposed that the use of bovine-bone powder eliminates the addition of thiols to obtain homogeneous size and shape particles. The use of bovine bone as catalytic support is rather novel. This synthesis method is of relatively low cost and environmentally friendly since the support is a waste material, the solvent is water, and the calcination step followed by reduction with hydrogen is eliminated. Moreover, the chemical structure of hydroxyapatite can form stable compounds and anchor the metal ions. The physical characteristics of hydroxyapatite allow its stirring, its stability at extreme pH, and its thermal stability.

Figure 3 shows the particles size distribution. The average diameter of synthesized nanoparticles was found to be 2.2 ± 0.6 nm.

Figure 4 shows a single nanoparticle with a 2.25 Å lattice planes, corresponding to the (111) plane of cubic metallic Pt [35]. Also, the external area of the support with a 2.72 Å lattice planes is observed. This corresponds to the (300) plane of hydroxyapatite [36]. Becerril-Juárez et al. [24] and Suber et al. [37] suggest that the growth of regular and symmetric nanostructures of metal nanoparticles appears to be controlled by a bimodal mechanism, including a thermodynamically driven diffusional growth as well as kinetically controlled aggregation process. The aggregation process along preferential directions appears to be kinetically controlled by a slow reduction of the metallic ions, which favours a crystalline and anisotropic aggregation. Conversely, a fast reduction may force the metallic nanoparticles to agglomerate in a polycrystalline but isotropic configuration. By observing the shape and chemical composition of the nanoparticles, the second mechanism appears to rule the synthesis of platinum nanoparticles with $NaBH_4$ as reducing agent since polycrystalline isotropic particles are obtained.

XPS was used to determine the oxidation state of the elements in the bovine-bone powder and the platinum nanoparticles. The narrow spectra in the Pt 4f region and its curve fitting show two oxidation states for platinum (Figure 5). The components at 70.9 eV ($4f_{7/2}$) and 74.1 eV ($4f_{5/2}$) can be attributed to metallic platinum in around 63% of the total platinum. The signals at 72.5 eV ($4f_{7/2}$) and 75.4 eV ($4f_{5/2}$) correspond to a 37% of the total platinum and can be ascribed to platinum oxide. These results indicate that the reduction of Pt (IV) to Pt° indeed took place and that Pt nanoparticles were supported onto the bovine-bone powder in controlled size and shape. Because of the aforesaid, the synthesized Pt nanoparticles/bovine-bone system is expected to exhibit catalytic activity in hydrogenation reactions. Therefore, to test this aspect the hydrogenation of an alkyne was selected.

The catalytic activity of the system Pt/bovine-bone was tested in the 2-butyne-1,4-diol hydrogenation reaction in a continuously stirred slurry reactor. Figure 6 shows a typical concentration-time profile of 2-butyne-1,4-diol hydrogenation using bovine-bone powder-Pt1% catalyst. The conversion of 2-butyne-1,4-diol was 100% after 3.5 hours. The catalytic activity is highly and positively correlated with the concentration of Pt metallic particles. Thus, by increasing the amount of PtO nanoparticles, its catalytic activity decreases. The highest attained selectivity of 2-butene-1,4-diol was 83% after 3 hours of reaction. As shown in Figure 6, the loss of selectivity can be ascribed to the appearance of the alkane and side products like crotyl alcohol and *n*-butanol.

Darder et al. [25] suggested that a H_2 pretreatment can improve the selectivity of the catalytic system; besides, higher H_2 pressure and higher temperature can improve the H_2 adsorption and the initial reaction rate. The optimization of such reaction variables will be the aim of future investigations.

Reaction Scheme 1 depicts the plausible mechanism of 2-butyne-1,4-diol hydrogenation attained with the synthesized catalyst. It is worth noticing that neither hydroxybutyraldehyde nor n-butyraldehyde was detected during reaction as expected with other catalytic systems. From Figure 6, it can be concluded that the loss of selectivity is mainly due to the appearance of the alkane according to reaction Scheme 1.

4. Conclusions

Bovine-bone powder is an efficient, low-cost support of platinum nanoparticles. The synthesis of this novel bionanocomposite is plausible by the direct reduction of the metallic salt and this method leads to obtaining 2.2 ± 0.6 nm metallic platinum nanoparticles. This synthesis method is of relatively

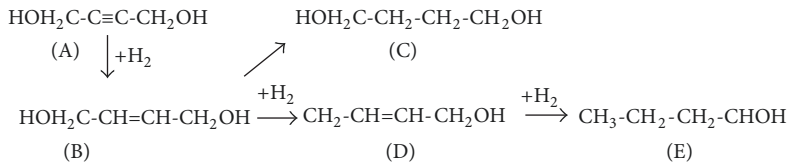

Scheme 1: 2-Butyne-1,4-diol hydrogenation scheme [29]. (A) 2-Butyne-1,4-diol, (B) 2-butene-1,4-diol, (C) butane-1,4-diol, (D) crotyl alcohol, and (E) n-butanol.

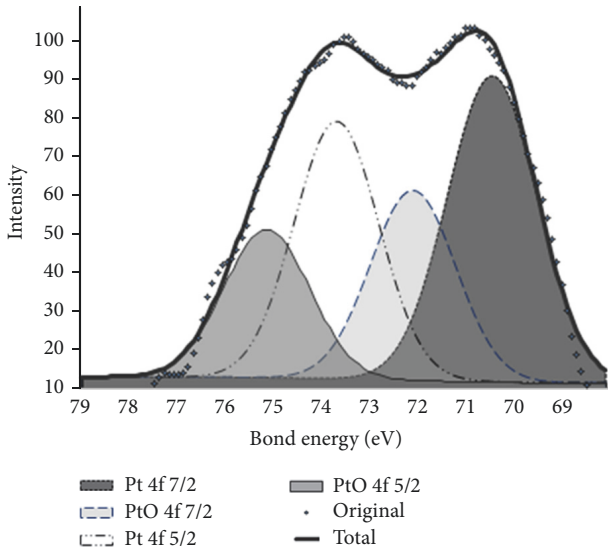

Figure 5: XPS spectra corresponding to the Pt 4f5/2 and 4f7/2 regions of the platinum nanoparticles supported over bovine-bone dust.

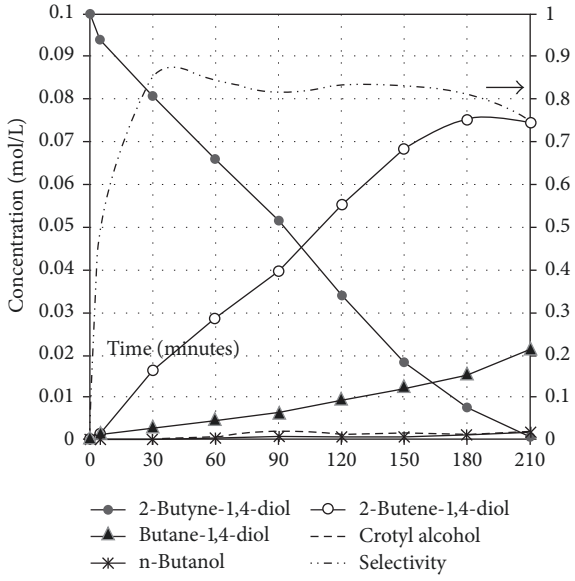

Figure 6: Concentration-time profile for 2-butyne-1,4-diol hydrogenation. Reaction conditions: temperature, 328 K; pressure, 6 bar; initial concentration = 0.1 mol/L; active concentration of catalyst, 0.215 mg; stirring speed, 550 rpm; total volume, 1.5×10^{-4} m^3.

low cost and environmentally friendly since the support is a waste material, the solvent is water, and the calcination step is eliminated. The platinum nanoparticles have electrostatic interactions with the hydroxyl group of the hydroxyapatite on the surface of the bovine-bone powder.

Finally, the system of bovine-bone powder with 1% platinum NPs possesses a high catalytic activity and selectivity for hydrogenation reactions. A nearly 100% conversion of 2-butyne-1,4-diol was achieved. The maximum attained selectivity towards 2-butene-1,4-diol was 83% at high conversions. This selectivity is mainly affected by the alkane presence.

Conflicts of Interest

The authors declare that they do not have conflicts of interest.

Acknowledgments

This project was supported by a grant from the National Institute on Minority Health and Health Disparities (G12MD007591) from the National Institutes of Health. Dr. Alfredo Rafael Vilchis-Nestor TEM imaging acquisition data at the Kleberg Advanced Microscopy Center of UTSA is acknowledged. The authors thank Dr. Gustavo López-Téllez (CCIQS, Universidad Autónoma del Estado de México) for assistance in XPS studies. S. A. Gama-Lara acknowledges CONACYT financial support to conduct postgraduate studies. CONACYT Project no. 269093 is also acknowledged.

References

[1] M. Wilson, *Nanotecnology: Basic Science and Emerging Technologies*, Chapman and Hall/ CRC, Boca Raton, Fla, USA, 1st edition, 2002.

[2] A. E. Hernández-Gómora, E. Lara-Carrillo, J. B. Robles-Navarro et al., "Biosynthesis of silver nanoparticles on orthodontic elastomeric modules: evaluation of mechanical and antibacterial properties," *Molecules*, vol. 22, no. 9, article no. 1407, 2017.

[3] U. Schubert, *Synthesis of Inorganic Materials*, Wiley-VCH, Weinheim, Germany, 2000.

[4] K. J. Klabunde, *Nanoscale Materials in Chemistry*, John Wiley and Sons, Inc., New York, NY, USA, 2001.

[5] P. Podsiadlo, S. Paternel, J.-M. Rouillard et al., "Layer-by-layer assembly of nacre-like nanostructured composites with antimicrobial properties," *Langmuir*, vol. 21, no. 25, pp. 11915–11921, 2005.

[6] E. Castro-Longoria, S. D. Moreno-Velásquez, A. R. Vilchis-Nestor, E. Arenas-Berumen, and M. Avalos-Borja, "Production of platinum nanoparticles and nanoaggregates using Neurospora crassa," *Journal of Microbiology and Biotechnology*, vol. 22, no. 7, pp. 1000–1004, 2012.

[7] A. R. Vilchis-Nestor, M. Avalos-Borja, S. A. Gómez, J. A. Hernández, A. Olivas, and T. A. Zepeda, "Alternative bio-reduction synthesis method for the preparation of Au(AgAu)/SiO2-Al2O3 catalysts: Oxidation and hydrogenation of CO," *Applied Catalysis B: Environmental*, vol. 90, no. 1-2, pp. 64–73, 2009.

[8] X. Zhang and Z. Su, "Polyelectrolyte-multilayer-supported Au@Ag core-shell nanoparticles with high catalytic activity," *Advanced Materials*, vol. 24, no. 33, pp. 4574–4577, 2012.

[9] V. Sanchez, R. Morales-Luckie, P. Garcia, and R. Lopez, "An aqueous phase synthetic route for ruthenium nanoparticles in cellulose nitrate fibres," *Material Letters*, vol. 62, pp. 2067–2070, 2007.

[10] Y. Zhang, S. Liu, W. Lu, and L. Wang, "In situ green synthesis of Au nanostructures on graphene oxide and their application for catalytic reduction of 4-nitrophenol," *Catalysis Science and Technology*, vol. 1, pp. 1142–1144, 2011.

[11] H. Wang, H. Y. Jeong, M. Imura et al., "Shape- and size-controlled synthesis in hard templates: Sophisticated chemical reduction for mesoporous monocrystalline platinum nanoparticles," *Journal of the American Chemical Society*, vol. 133, no. 37, pp. 14526–14529, 2011.

[12] I. Alonso-Lemus, Y. Verde-Gómez, and L. Álvarez-Contreras, "Platinum nanoparticles synthesis supported in mesoporous silica and its effect in MCM-41 lattice," *International Journal of Electrochemical Science*, vol. 6, pp. 4176–4187, 2011.

[13] L. Kong, G. Duan, and G. Zuo, "Rattle-type Au@TiO_2 hollow microspheres with multiple nanocores and porous shells and their structurally enhanced catalysis," *Materials Chemistry and Physics*, vol. 123, no. 2-3, pp. 421–426, 2010.

[14] L. Ouyang, D. M. Dotzauer, S. R. Hogg, J. MacAnás, J.-F. Lahitte, and M. L. Bruening, "Catalytic hollow fiber membranes prepared using layer-by-layer adsorption of polyelectrolytes and metal nanoparticles," *Catalysis Today*, vol. 156, no. 3-4, pp. 100–106, 2010.

[15] G. Yang, Y. Li, R. Rana, and J. Zhu, "Pt–Au/nitrogen-doped graphene nanocomposites for enhanced electrochemical activities," *Journal of Materials Chemistry A*, vol. 1, pp. 1754–1762, 2013.

[16] Y. Zhang, D. Kang, C. Saquing, M. Aindow, and C. Erkey, "Supported platinum nanoparticles by supercritical deposition," *Industrial and Engineering Chemistry Research*, vol. 44, no. 11, pp. 4161–4164, 2005.

[17] X. Huang, C. Guo, J. Zuo, N. Zheng, and G. D. Stucky, "An assembly route to inorganic catalytic nanoreactors containing sub-10-nm gold nanoparticles with anti-aggregation properties," *Small*, vol. 5, no. 3, pp. 361–365, 2009.

[18] S. Zhang, Y. Shao, H.-G. Liao et al., "Graphene decorated with PtAu alloy nanoparticles: facile synthesis and promising application for formic acid oxidation," *Chemistry of Materials*, vol. 23, no. 5, pp. 1079–1081, 2011.

[19] F. E. Meva, C. O. Ebongue, S. V. Fannang et al., "Natural Substances for the Synthesis of Silver Nanoparticles against Escherichia coli: The Case of Megaphrynium macrostachyum (Marantaceae), Corchorus olitorus (Tiliaceae), Ricinodendron heudelotii (Euphorbiaceae), Gnetum bucholzianum (Gnetaceae), and Ipomoea batatas (Convolvulaceae)," *Journal of Nanomaterials*, vol. 2017, Article ID 6834726, 6 pages, 2017.

[20] R. A. Morales-Luckie, A. A. Lopezfuentes-Ruiz, O. F. Olea-Mejía et al., "Synthesis of silver nanoparticles using aqueous extracts of Heterotheca inuloides as reducing agent and natural fibers as templates: Agave lechuguilla and silk," *Materials Science and Engineering C: Materials for Biological Applications*, vol. 69, pp. 429–436, 2016.

[21] E. R. Balasooriya, C. D. Jayasinghe, U. A. Jayawardena, R. W. D. Ruwanthika, R. M. De Silva, and P. V. Udagama, "Honey mediated green synthesis of nanoparticles: new era of safe nanotechnology," *Journal of Nanomaterials*, vol. 2017, Article ID 5919836, 10 pages, 2017.

[22] Y. Yulizar, T. Utari, H. A. Ariyanta, and D. Maulina, "Green method for synthesis of gold nanoparticles using polyscias scutellaria leaf extract under uv light and their catalytic activity to reduce methylene blue," *Journal of Nanomaterials*, pp. 1–6, 2017.

[23] L. Yumei, L. Yamei, L. Qiang, and B. Jie, "Rapid biosynthesis of silver nanoparticles based on flocculation and reduction of an exopolysaccharide from arthrobacter sp. B4: its antimicrobial activity and phytotoxicity," *Journal of Nanomaterials*, vol. 2017, Article ID 9703614, 8 pages, 2017.

[24] I. G. Becerril-Juárez, R. A. Morales-Luckie, F. Ureña-Nuñez, J. A. Arenas-Alatorre, J. P. Hinestroza, and V. Sánchez-Mendieta, "Silver micro-, submicro- and nano-crystals using bovine bone as template. Formation of a silver/bovine bone composite," *Materials Letters*, vol. 85, pp. 157–160, 2012.

[25] M. Darder, P. Aranda, and E. Ruiz-Hitzky, "Bionanocomposites: A new concept of ecological, bioinspired, and functional hybrid materials," *Advanced Materials*, vol. 19, no. 10, pp. 1309–1319, 2007.

[26] X. Lin, M. Wu, D. Wu, S. Kuga, T. Endo, and Y. Huang, "Platinum nanoparticles using wood nanomaterials: Eco-friendly synthesis, shape control and catalytic activity for p-nitrophenol reduction," *Green Chemistry*, vol. 13, no. 10, pp. 283–287, 2011.

[27] L. B. Devi and A. B. Mandal, "Self-assembly of Ag nanoparticles using hydroxypropyl cyclodextrin: Synthesis, characterisation and application for the catalytic reduction of p-nitrophenol," *RSC Advances*, vol. 3, no. 15, pp. 5238–5253, 2013.

[28] J. He, T. Kunitake, and A. Nakao, "Facile in situ synthesis of noble metal nanoparticles in porous cellulose fibers," *Chemistry of Materials*, vol. 15, no. 23, pp. 4401–4406, 2003.

[29] R. Natividad, R. Kulkarni, K. Nuithitikul, S. Raymahasay, J. Wood, and J. M. Winterbottom, "Analysis of the performance of single capillary and multiple capillary (monolith) reactors for the multiphase Pd-catalyzed hydrogenation of 2-butyne-1,4-diol," *Chemical Engineering Science*, vol. 59, no. 22-23, pp. 5431–5438, 2004.

[30] A. B. Mandal, D. V. Ramesh, and S. C. Dhar, "Physico-chemical studies of micelle formation on sepia cartilage collagen solutions in acetate buffer and its interaction with ionic and non-ionic micelles. Hydrodynamic and thermodynamic studies," *European Journal of Biochemistry*, vol. 169, no. 3, pp. 617–628, 1987.

[31] R. P. Fishwick, R. Natividad, R. Kulkarni et al., "Selective hydrogenation reactions: a comparative study of monolith CDC, stirred tank and trickle bed reactors," *Catalysis Today*, vol. 128, no. 1-2, pp. 108–114, 2007.

[32] M. M. Telkar, C. V. Rode, R. Jaganathan, V. H. Rane, and R. V. Chaudhari, "Platinum catalyzed hydrogenation of 2-butyne-1,4-diol," *Journal of Molecular Catalysis A: Chemical*, vol. 187, no. 1, pp. 81–93, 2002.

[33] R. A. Morales-Luckie, V. Sanchez-Mendieta, J. A. Arenas-Alatorre et al., "One-step aqueous synthesis of stoichiometric Fe-Cu nanoalloy," *Materials Letters*, vol. 62, no. 26, pp. 4195–4197, 2008.

[34] Y. Mei, G. Sharma, Y. Lu et al., "High catalytic activity of platinum nanoparticles immobilized on spherical polyelectrolyte brushes," *Langmuir*, vol. 21, no. 26, pp. 12229–12234, 2005.

[35] ICDD, International Center for Diffraction Data, File (PDF) Pt #00-004-0802, 2002.

[36] E. Domashevskaya, A. Al-Zubaidi, D. Goloshchapov, N. Rumyantseva, and P. Seredin, "Study of metal substituted calcium deficient hydroxyapatite," *Condensed Matter and Interphase Boundaries*, vol. 16, pp. 134–141, 2014.

[37] L. Suber, I. Sondi, E. Matijević, and D. V. Goia, "Preparation and the mechanisms of formation of silver particles of different morphologies in homogeneous solutions," *Journal of Colloid and Interface Science*, vol. 288, no. 2, pp. 489–495, 2005.